ARTICLE

Mutations in *WNT1* Cause Different Forms of Bone Fragility

Katharina Keupp,[1,2,3] Filippo Beleggia,[1,2,3] Hülya Kayserili,[4] Aileen M. Barnes,[5] Magdalena Steiner,[6] Oliver Semler,[7] Björn Fischer,[6] Gökhan Yigit,[1,2,3] Claudia Y. Janda,[8] Jutta Becker,[1] Stefan Breer,[9] Umut Altunoglu,[4] Johannes Grünhagen,[6] Peter Krawitz,[6] Jochen Hecht,[10] Thorsten Schinke,[9] Elena Makareeva,[11] Ekkehart Lausch,[12] Tufan Cankaya,[13] José A. Caparrós-Martín,[14,15] Pablo Lapunzina,[15,16] Samia Temtamy,[17] Mona Aglan,[17] Bernhard Zabel,[12] Peer Eysel,[18] Friederike Koerber,[19] Sergey Leikin,[11] K. Christopher Garcia,[8] Christian Netzer,[1] Eckhard Schönau,[7] Victor L. Ruiz-Perez,[14,15] Stefan Mundlos,[6,20] Michael Amling,[9] Uwe Kornak,[6,20,*] Joan Marini,[5] and Bernd Wollnik[1,2,3,*]

We report that hypofunctional alleles of *WNT1* cause autosomal-recessive osteogenesis imperfecta, a congenital disorder characterized by reduced bone mass and recurrent fractures. In consanguineous families, we identified five homozygous mutations in *WNT1*: one frameshift mutation, two missense mutations, one splice-site mutation, and one nonsense mutation. In addition, in a family affected by dominantly inherited early-onset osteoporosis, a heterozygous *WNT1* missense mutation was identified in affected individuals. Initial functional analysis revealed that altered WNT1 proteins fail to activate canonical LRP5-mediated WNT-regulated β-catenin signaling. Furthermore, osteoblasts cultured in vitro showed enhanced *Wnt1* expression with advancing differentiation, indicating a role of WNT1 in osteoblast function and bone development. Our finding that homozygous and heterozygous variants in *WNT1* predispose to low-bone-mass phenotypes might advance the development of more effective therapeutic strategies for congenital forms of bone fragility, as well as for common forms of age-related osteoporosis.

Introduction

Osteogenesis imperfecta (OI) is a monogenic disease primarily characterized by dramatically increased bone fragility and—in most cases—low bone mass.[1] The phenotypic spectrum of OI ranges from very mild forms up to severe and lethal types of the disease. The majority of OI cases are inherited in an autosomal-dominant manner and are caused by mutations in *COL1A1* (MIM 120150) and *COL1A2* (MIM 120160), encoding the two α chains of collagen type I, the predominant protein component of the bone matrix.[2] Autosomal-recessive inheritance has also been described in nearly 10% of all OI cases. In this form of OI, several causative mutations have been identified in genes encoding mainly proteins involved in collagen type I folding, modification, or matrix mineralization. To date, mutations in the following genes have been described to cause recessively inherited forms of OI: *CRTAP*[3] (MIM 605497), *LEPRE1*[4] (MIM 610339), *SERPINH1*[5] (MIM 600943), *PPIB*[6] (MIM 123841), *SP7*[7] (MIM 606633), *SERPINF1*[8] (MIM 172860), *FKBP10*[9] (MIM 607063), *BMP1*[10,11] (MIM 112264), *TMEM38B*[12] (MIM 611236), and *PLOD2* (MIM 601865).[13]

Direct or indirect collagen defects result in defective bone-matrix formation and mineralization and consequently lead to impaired bone flexibility and integrity of the skeletal system. However, collagen type I sequence variants have been associated with reduced bone mass and bone fragility not only in individuals suffering from congenital OI but also in individuals with age-related osteoporosis.[14] Osteoporosis is a very common disease affecting the skeletal system and is characterized by reduced bone mineral density and increased fracture risk. In contrast to that of OI, the pathophysiology of osteoporosis is thought to result from a bone-homeostasis imbalance based on a disturbed balance of osteoblast and

[1]Institute of Human Genetics, University Hospital Cologne, University of Cologne, 50931 Cologne, Germany; [2]Center for Molecular Medicine Cologne, University of Cologne, 50931 Cologne, Germany; [3]Cologne Excellence Cluster on Cellular Stress Responses in Aging-Associated Diseases, University of Cologne, 50931 Cologne, Germany; [4]Medical Genetics Department, Istanbul Medical Faculty, Istanbul University, 34093 Istanbul, Turkey; [5]Bone and Extracellular Matrix Branch, National Institute of Child Health and Human Development, National Institutes of Health, Bethesda, MD 20892, USA; [6]Institute of Medical Genetics and Human Genetics, Charité-Universitätsmedizin Berlin, 13353 Berlin, Germany; [7]Children's Hospital, University of Cologne, 50931 Cologne, Germany; [8]Department of Molecular and Cellular Physiology and Department of Structural Biology, Howard Hughes Medical Institute, Stanford University School of Medicine, Stanford, CA 94305, USA; [9]Department of Osteology and Biomechanics, University Medical Center Hamburg-Eppendorf, 20246 Hamburg, Germany; [10]Berlin-Brandenburg Centre for Regenerative Therapies, 13353 Berlin, Germany; [11]Section on Physical Biochemistry, National Institute of Child Health and Human Development, National Institutes of Health, Bethesda, MD 20892, USA; [12]Division of Genetics, Children's Hospital, University of Freiburg, 79106 Freiburg, Germany; [13]Department of Medical Genetics, Dokuz Eylul University Medical Faculty, 35210 Izmir, Turkey; [14]Instituto de Investigaciones Biomédicas, Consejo Superior de Investigaciones Científicas and Universidad Autónoma de Madrid, 28029 Madrid, Spain; [15]Centro de Investigación Biomédica en Red de Enfermedades Raras, Instituto de Salud Carlos III, 28029 Madrid, Spain; [16]Instituto de Genética Médica y Molecular, Instituto de Investigación Hospital Universitario La Paz, Universidad Autónoma de Madrid, 28046 Madrid, Spain; [17]Human Genetics and Genome Research Division, National Research Centre, El-Buhouth Street, Dokki, 12311 Cairo, Egypt; [18]Department of Orthopaedic and Trauma Surgery, University of Cologne, 50931 Cologne, Germany; [19]Department of Radiology, University of Cologne, 50931 Cologne, Germany; [20]Max Planck Institute for Molecular Genetics, 14195 Berlin, Germany
*Correspondence: bwollnik@uni-koeln.de (B.W.), uwe.kornak@charite.de (U.K.)
http://dx.doi.org/10.1016/j.ajhg.2013.02.010.

osteoclast function.[15,16] Common age-related osteoporosis represents a multifactorial disease to which contributes a combination of predisposing genetic and environmental factors. The identification of genes underlying monogenic diseases with altered bone mass has substantially increased our knowledge of the key factors and pathways responsible for skeletal development and bone homeostasis, as well as pathogenic mechanisms predisposing to recurrent fractures.[1,16,17] This understanding is essential to the development of new effective therapies for common disorders, such as osteoporosis.[18] Recently, mutations in *LRP5* (MIM 603506) and other factors involved in WNT-regulated β-catenin signaling have been shown to cause disorders with abnormal bone mass, suggesting an important role for this pathway in the regulation of bone homeostasis.[19–21]

Here, we present genetic and functional evidence that mutations in *WNT1* cause different forms of bone fragility. We show that homozygous loss-of-function mutations underlie autosomal-recessive OI and that a heterozygous *WNT1* mutation was inherited in an autosomal-dominant pattern in a family with early-onset osteoporosis. Hence, WNT1 plays a crucial role in bone formation and bone-remodeling processes, and this finding might facilitate the use of more effective therapeutic strategies.

Material and Methods

Subjects

All subjects or their legal representatives gave written informed consent to the study. The study was performed in accordance with the Declaration of Helsinki protocols and was approved by the local institutional review boards. DNA from participating family members was extracted from peripheral-blood lymphocytes by standard extraction procedures.

XtremeCT

Analysis of bone microarchitecture of the nondominant distal radius was performed by high-resolution peripheral quantitative computed tomography (CT) (XtremeCT, Scanco Medical, Brüttisellen, Switzerland) on five adults from a family affected by a dominant heterozygous c.703C>T (p.Arg235Trp) mutation in *WNT1*. The distal forearm of each affected individual was immobilized in a carbon-fiber shell for the reduction of motion artifacts. Afterward, the shell was fixed to the scanner and scanned as previously described.[22] An anteroposterior scout view was performed for identifying the region of interest. Afterward, the reference line was set at the endplate of the radius, and the measurement started 9.5 mm proximal to the manually set reference line. Subsequently, 110 CT slices—representing approximately 9 mm in the axial direction—were obtained. Thus, we were able to analyze relative bone volume (BV/TV), trabecular thickness (Tb.Th), cortical thickness (Ct.Th), and cortical density (D_{cort}).

Next-Generation Sequencing

Exonic and adjacent intronic sequences were enriched from genomic DNA with the use of the Agilent SureSelect Human Exome Kit and were run on the Illumina Genome Analyzer IIX Sequencer by Oxford Gene Technology and on the Illumina HiSeq 2000 Sequencer from the Max Planck Institute for Molecular Genetics. Alignment was performed with the Burrows-Wheeler Aligner, and PCR duplicates were marked with Picard tools. Local realignment around indels, base-quality recalibration, and variant calling were performed with the Genome Analysis Toolkit. The resulting variants were annotated with Annovar and filtered according to their genomic position, predicted effect, and frequency in the general population from dbSNP, the 1000 Genomes Project, the National Heart, Lung, and Blood Institute (NHLBI) Exome Sequencing Project Exome Variant Server (EVS), and our in-house database. Homozygous regions were defined with an in-house script based on a hidden Markov model and on the Viterbi algorithm with the use of variants found in the whole-exome sequencing (WES) data and loci of known polymorphisms from dbSNP. After initial discovery of the disease-causing mutation, additional exome-sequencing data were analyzed with the GeneTalk platform.[23]

mRNA Analysis of *WNT1* Transcripts

RNA of the affected individual was extracted from fresh blood with the Paxgene Blood RNA system (QIAGEN, Hilden, Germany). RT-PCR was performed via RevertAid First Strand cDNA Synthesis Kit (Thermo Scientific, Schwerte, Germany). RT-PCR products were used for *WNT1*-specific PCR amplification. The complete open reading frame (1,113 bp) of *WNT1* was amplified with primers 5′-ATGGGGCTCTGGGCGCTGTTG-3′ (forward) and 5′-TCACA GACACTCGTGCAGTAC-3′ (reverse) and was separated on 1% agarose gel. The PCR product of this cDNA showed a dramatically reduced amount of *WNT1* transcripts.

Generation of *WNT1* Constructs

The coding sequence of human *WNT1* cDNA (RefSeq accession number NM_005430.3) was cloned into the pCDNA3 expression vector. The mutant variants of *WNT1* were generated by site-directed mutagenesis with a primer containing the specific nucleotide substitutions. The cDNA sequences of all constructs were confirmed by Sanger sequencing.

Modeling of *WNT1* Mutations

The WNT1 substitutions p.Gly177Cys and p.Arg235Trp are positioned within regions of conserved secondary structure, restricted by conserved disulfide bonds, and surrounded by conserved amino acids between XWnt8 and WNT1, making structure-based manual modeling into the XWnt8 structure (pdb 4F0A) the method of choice and prediction reliable. For modeling the p.Gly177Cys and p.Arg235Trp substitutions into the XWnt8 structure, the corresponding side chains of the WNT1 changes and the nearby residues, which differ between XWnt8 and WNT1 (e.g., Thr136, Val139, Glu217), were built manually in COOT,[24,25] and clashes were inspected with MolProbity. Rotamers shown in Figure 5 produced the fewest clashes.

Luciferase Assay

Human embryonic kidney (HEK) 293T cells cultured in Dulbecco's modified Eagle's medium containing 10% fetal bovine serum (Life Technologies, Darmstadt, Germany) and antibiotics were plated in 24-well plates 18 hr prior to transfection. Transient transfections were performed in triplicate with FuGeneHD (Roche, Mannheim, Germany) according to the manufacturer's

instruction with the following expression constructs: wild-type (WT) *WNT1* and mutant variants of *WNT1* (200 ng), *LRP5* (200 ng), *MESDC2* (80 ng), Topflash (100 ng), and pRL-TK (5 ng). For ensuring equal amounts of DNA, 200 ng *LacZ*-pCDNA3.1 was used in *WNT1*-negative transfections. Thirty hours after transfection, cells were lysed and frozen in lysis buffer overnight at −20°C so that lysing efficiency would increase. After thawing, luciferase activity was measured with a Dual-Luciferase Reporter Assay Kit (Promega, Mannheim, Germany) and a Glomex 96-microplate luminometer. Each transfection was measured in triplicate.

Osteoblast Culture

Primary mouse osteoblasts were obtained by sequential collagenase digestion of calvariae from newborn C57/BL6 WT mice. Cells were seeded at high density on 6-well plates in alpha minimum essential medium (MEM) (Lonza, Cologne, Germany) containing 10% fetal calf serum (Life Technologies, Darmstadt, Germany), Pen/Strep (Lonza, Cologne, Germany), and 2 mM UltraGlutamine (Lonza, Cologne, Germany). When cells reached confluence, alpha MEM was supplemented with 50 μM L-ascorbate-2-phosphate (Sigma, Steinheim, Germany) and 10 mM beta glycerophosphate (Sigma, Steinheim, Germany) for inducing osteoblast differentiation. Osteoblasts started forming visible mineral deposition at day 9. Every 3 days, RNA was isolated with RNA-Pure (Peqlab, Erlangen, Germany).

Expression Analysis

Tissue specimens were shock frozen in liquid nitrogen after dissection. After pulverization, RNA was isolated with the Trizol (Life Technologies, Darmstadt, Germany) method. Total cDNA from tissue or cultured osteoblasts was transcribed by the RevertAidTM H Minus First Strand cDNA Synthesis Kit (Fermentas, St. Leon-Rot, Germany) with random hexamer primer. Quantitative PCR was performed with EvaGreen (Solis Biodyne, Tartu, Estonia) on ABI Prism 7500 (Applied Biosystems, Foster City, CA, USA). Data were analyzed by the ABI Prism SDS Software package according to the cycle-threshold method with the use of *GAPDH* expression as a reference. All primer sequences are available upon request.

Results

A Homozygous *WNT1* Mutation Causes OI in a Large Turkish Family

We examined a consanguineous Turkish family (family 1) with three affected individuals diagnosed with OI in two different branches of the family (Figure 1A). Affected individuals showed typical clinical OI features, including early-onset recurrent fractures (Figure 1B), bone deformity, significant reduction of bone density, short stature, and bluish sclerae in some of the affected individuals. Tooth development and hearing were normal (Table 1). After exclusion of all described genes for autosomal-recessive OI by haplotyping or direct sequencing, we performed WES in affected person V:1 of the family. For WES data analysis, we applied a combination of determining homozygous stretches with all WES variants and filtering for novel and likely protein-affecting variants. By this filtering strategy, we reduced the number of likely causative variants to 11, and all of them were located within the ten largest stretches of homozygosity (Tables S1–S3, available online). These variants were not annotated in dbSNP132, the 1000 Genomes Database, or the EVS.

The only variant predicted to be functionally detrimental was a homozygous 1 bp duplication, c.859dupC in *WNT1* (RefSeq NM_005430.3, MIM 164820), located within a large homozygous region in 12q13 (Figure S1 and Table S2). Sanger sequencing and microsatellite-marker analysis confirmed cosegregation of the mutation and the disease-causing haplotype. All affected individuals are homozygous for the c.859dupC mutation, whereas their parents are heterozygous carriers (Figure 2A and Figure S1). The 1 bp duplication in *WNT1* is predicted to lead to a frameshift and early truncation of the C-terminal part of the protein (p.His287Profs*30).

Mutational Spectrum of *WNT1* in Autosomal-Recessive OI

Sequencing of the entire *WNT1* coding region in 11 additional autosomal-recessive-OI-affected families, for which all known genes affected in OI had been excluded, identified four additional homozygous mutations in consanguineous OI-affected families (Figure 1A and Table 1): two missense mutations (c.529G>T [p.Gly177Cys] and c.893T>G [p.Phe298Cys]), an exon 3 donor-splice-site mutation (c.624+4A>G), and a nonsense mutation (c.565G>T [p.Glu189*]; RefSeq NM_005430.3) (Figure 2A). We used cDNA from the affected individual carrying the putative donor-splice-site mutation c.624+4A>G to verify the effect of the mutation on splicing of the *WNT1* transcript. Interestingly, we observed that, compared to the control, the mutation caused a dramatic reduction in normal *WNT1* transcripts. This result suggests that the c.624+4A>G mutant transcripts might be unstable and degraded by nonsense-mediated mRNA decay (Figure 2B). The c.529G>T mutation substitutes the highly conserved glycine at position 177 to cysteine, whereas the c.893T>G mutation leads to the substitution of a cysteine for a phenylalanine at position 298 (Figures 2A, 2C, and 2D). None of the identified mutations are listed in >13,000 alleles of the EVS. Our genetic data establish recessive mutations in *WNT1* as a cause of autosomal-recessive OI.

Interestingly, we observed different clinical severity of the phenotype in OI caused by *WNT1* mutation; it ranged from moderate to progressively deforming forms, which can occasionally lead to early infant death (Figures 1B–1D and Table 1).

A Dominant *WNT1* Mutation Causes Early-Onset Osteoporosis

Concurrently, WES of two affected individuals from a four-generation family (Figure 3A) affected by early-onset osteoporosis and fractures inherited in an autosomal-dominant pattern revealed no mutations in described

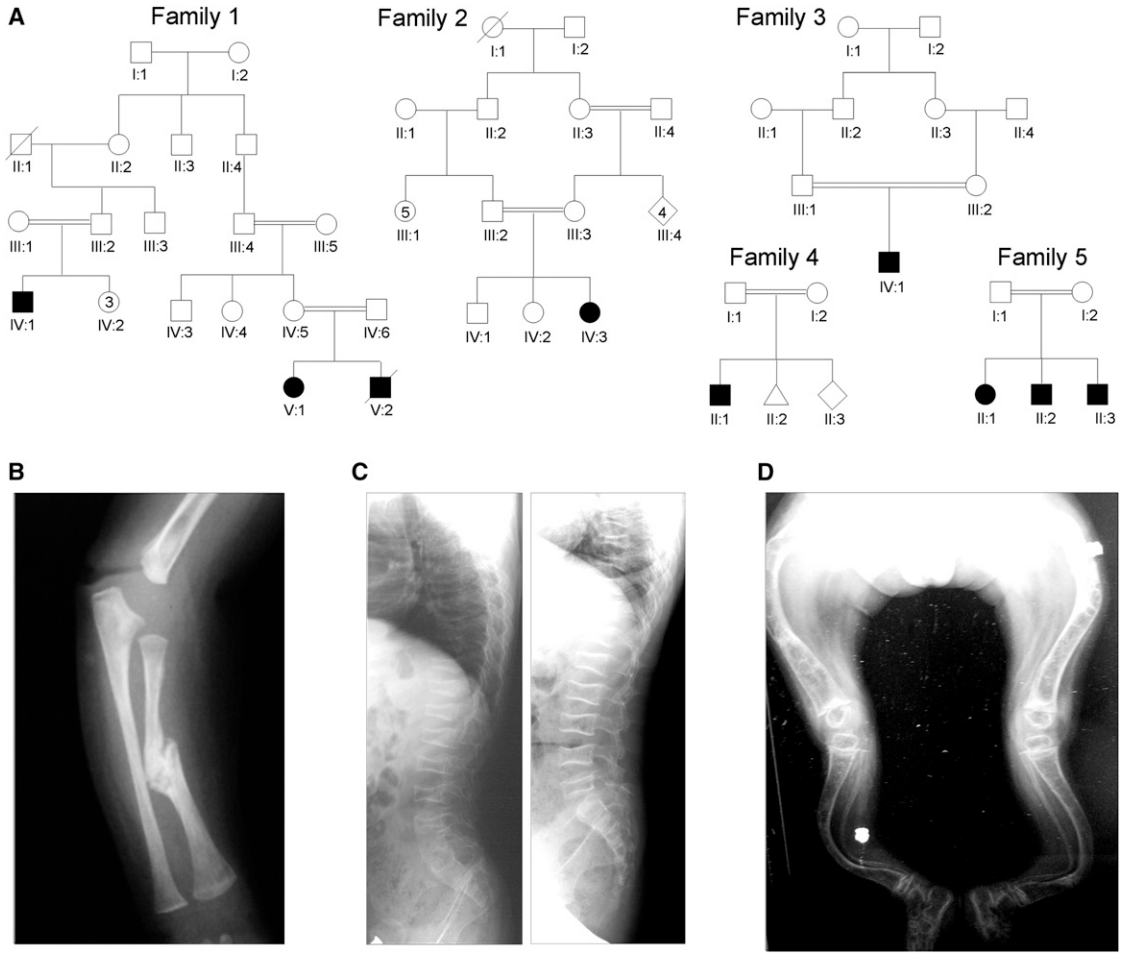

Figure 1. Families Affected by Autosomal-Recessive OI
(A) Pedigrees of four Turkish families (families 1–4) and one Egyptian family (family 5) affected by autosomal-recessive OI. WES was done on DNA from affected member V:1 of family 1.
(B) X-rays of family 1 individual IV:1, who harbors the homozygous p.His287Profs*30 WNT1 variant, show a fracture.
(C) Lateral spine X-rays of the family 2 member with the homozygous WNT1 p.Gly177Cys substitution. An X-ray was taken at the start of treatment with bisphosphonates (left). The vertebrae are severely compressed and deformed, and even after 4 years of treatment with bisphosphonates, no improvement in size or shape is visible in the lumbar spine (right).
(D) An X-ray of individual II:3 (family 5), who has p.Phe298Cys in WNT1, shows severe deformities of the legs.

genes affecting bone mass but did reveal that the heterozygous c.703C>T variant in *WNT1* segregates with the phenotype in the family (Figures 3A and 3B). This mutation is predicted to lead to a substitution of the arginine at position 235 to tryptophan (p.Arg235Trp). This variant is not found in over 13,000 alleles listed in the EVS. Affected family members clinically showed recurrent fractures (for example, of vertebrae and ribs after minor trauma beginning in adolescence), low-bone-turnover markers, and a reduction of trabecular and cortical bone as revealed by high-resolution CT (Figure 3C and Table S4). Interestingly, when performing bone-density measurements in parents of two of our recessive OI cases, we found that one father harboring the heterozygous c.859dupC (p.His287Profs*30) mutation showed signs of early-onset osteoporosis at the age of 42 years, whereas bone density was in the lower normal ranges in the other parents.

Functional In Vitro Effects of Identified *WNT1* Mutations

To examine whether the identified *WNT1* mutations have compromising effects on canonical WNT-regulated β-catenin signaling transduction, we performed a dual luciferase reporter assay. Here, we used the TOPFlash vector as a reporter containing the coding sequence of firefly luciferase downstream of TCF binding sites. The canonical WNT-mediated signal triggers the expression of firefly luciferase, and the enzymatic activity of luciferase can be quantified. Initially, we showed that WT WNT1 can bind LRP5 and activate WNT-regulated β-catenin signaling (Figure 4). Subsequently, coexpression of LRP5 and constructs encoding the p.Gly177Cys, p.His287Profs*30, and p.Arg235Trp variants showed a significant reduction in luciferase activity in this in vitro assay. This result clearly indicates that all three tested mutations almost completely fail to activate the WNT-regulated β-catenin signaling cascade (Figure 4).

Table 1. Clinical Findings in Individuals with Autosomal-Recessive OI

	Family 1			Family 2	Family 3	Family 4	Family 5		
	IV:1	V:1	V:2	IV:3	IV:1	II:1	II:1	II:2	II:3
Sex	male	female	male	female	male	male	female	male	male
Disease severity	moderate	moderate	severe (exitus at 5 months of age)	moderate	severe	severe	severe	severe	severe
Skeletal Findings									
Multiple fractures of extremities	yes	yes	yes	yes	yes	yes	yes	yes	yes
Age at first fracture (months)	3	1 day after birth	in utero	2	7	in utero	3 days after birth	1	10 days after birth
Vertebral fractures	no	no	no	yes	yes	yes	no	no	no
Bowing of upper extremities	yes	no	yes	no	no	yes	yes	yes	yes
Bowing of lower extremities	yes	yes	no	yes	yes	yes	yes	yes	yes
Shortening of upper extremities	yes	no	no	no	no	yes	yes	yes	yes
Shortening of lower extremities	yes	no	no	yes	yes	yes	yes	yes	yes
Other Findings									
Color of sclera	white	bluish gray	blue	blue	white	white	faint blue	faint blue	blue
Dentinogenesis imperfecta	no	no	no	no	no	no	no	no	no
Hypermobility of joints	no	no	no	no	no	no	yes	yes	yes
Cardiac impairment	no	no	no	no	no	no	no	no	no
Hearing impairment	no	no	no	no	no	no	no	no	no
Intellectual development	normal	normal	delayed	normal	normal	normal	normal	normal	normal
Therapy									
Bisphosphonate treatment	no	yes	no	yes	yes	yes	yes	yes	yes
Molecular basis									
WNT1 alteration	p.His287Profs*30	p.His287Profs*30	p.His287Profs*30[a]	p.Gly177Cys	c.624+4A>G	p.Glu189*	p.Phe298Cys	p.Phe298Cys	p.Phe298Cys

[a]Caused by a familial mutation; DNA not available for testing.

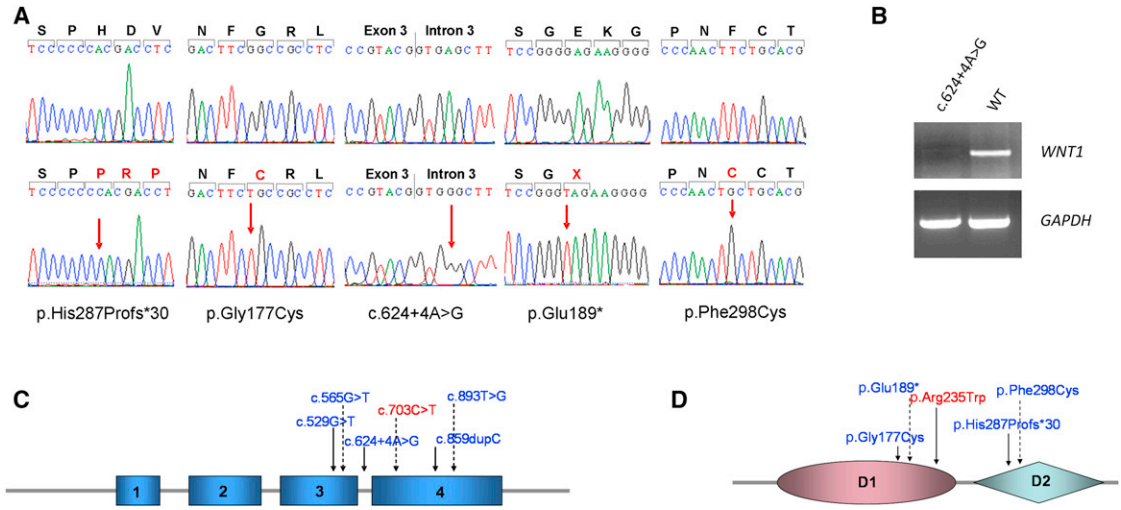

Figure 2. Homozygous Mutations in *WNT1* in Autosomal-Recessive Families
(A) Chromatograms of identified recessive *WNT1* mutations (red arrows) in comparison to the respective sequence.
(B) mRNA analysis of *WNT1* transcripts in the affected individual harboring the homozygous c.624+4A>G splice-site mutation. The PCR product of analyzed cDNA shows a drastically reduced amount of *WNT1* transcripts.
(C and D) A schematic genomic overview of *WNT1* (C) and WNT1 (D) indicates the localization of the identified *WNT1* mutations. WNT1 domains were predicted on the crystal structure of XWnt8.

Structural Effects of *WNT1* Mutations in a Protein Model

In order to gain insights into the pathogenic effects of dominant and recessive *WNT1* missense mutations, we modeled the recessive p.Gly177Cys and dominant p.Arg235Trp substitutions on the crystal structure of XWnt8, which has been recently described.[26] Gly at position 177 is highly conserved in human WNTs in order to allow close packing of helices C and D within the WNT 7-helix bundle (Figure 5). In the p.Gly177Cys substitution, the side chain of Cys177 would point into the core of the helical bundle (within the interface to helix D), resulting in separation of the close van der Waals packing within this helical core. This disruption of the tight packing would most likely lead to destabilization and perhaps to unfolding of the WNT1 core, which is thought to be responsible for binding to LRP5/6 (Figure 5).

Arg235 is located within the β-stand B at the base of the lipid-modified β-hairpin and is surrounded by residues conserved between WNT1 and XWnt8. In human WNTs, position 235 is occupied by either small amino acids or amino acids with long and flexible side chains and is surrounded by several other well-structured amino acids. The Trp side chain in the p.Arg235Trp mutant would clash with the side chains of Trp233, Arg141, and Asp172 and probably disrupt the structure of WNT1's thumb region, which seems to be important for interaction with FZ proteins (Figure 5). In summary, both missense changes are predicted to disturb the formation of the LRP5/6-WNT1-FZ complex.

Wnt1 Expression in Osteoblasts

Wnt1 is known to be strongly expressed during neuronal development, and its complete inactivation in knockout mice leads to a lethal phenotype as a result of malformation of the midbrain and cerebellum.[27] To examine expression of *Wnt1* in the osteoblast lineage, we used quantitative PCR to measure mRNA levels in cultured calvarial osteoblasts and found enhanced *Wnt1* expression with advancing differentiation. The efficient differentiation was confirmed by the expression of osterix (*Sp7*) and sclerostin (*Sost*), which are marker genes for osteoblasts and terminally differentiated osteoblasts, respectively (Figure 6A). Furthermore, *Wnt1* expression increased in postnatal compared to embryonic long bones (Figure 6B). This might indicate that in the bone compartment, WNT1 influences the osteoblast lineage itself or some adjacent cell type.

Discussion

We report that hypofunctional alleles of *WNT1* cause low-bone-mass phenotypes in humans. Whereas recessively inherited reduction in WNT1 function underlies congenital OI, the fact that a heterozygous *WNT1* mutation predisposes to early-onset osteoporosis implies a dominant effect. Altered WNT1 proteins lose the ability to activate LRP5-mediated WNT-regulated β-catenin signaling in vitro. Although this demonstrates the functional effects of the mutations, it is currently not clear whether WNT1 also interacts with LRP5 in vivo. In order to gain more insights into the functional difference of recessive versus dominant missense mutation, we modeled both mutations on the crystal structure of XWnt8.[26] One plausible scenario why the p.Arg235Trp variant acts dominantly is that p.Arg235Trp destabilizes the β-stand that supports the lipid containing the "site 1" Fz-CRD binding loop.

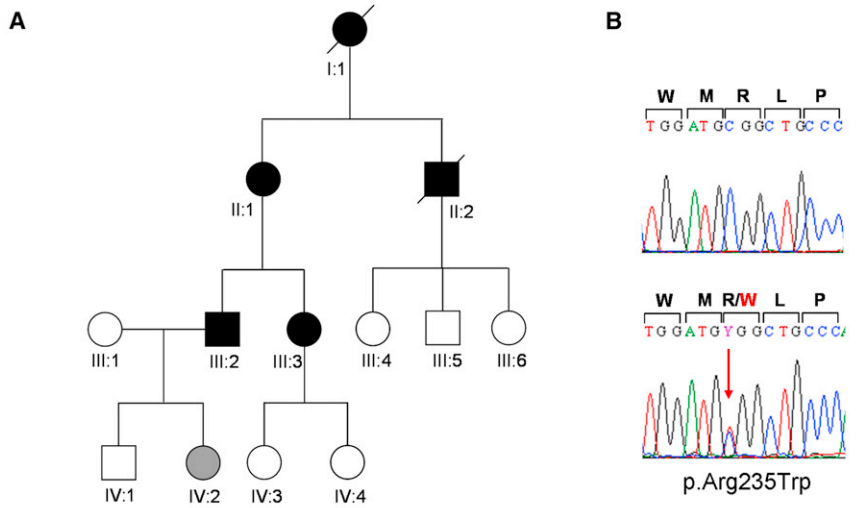

Figure 3. A Dominant *WNT1* Mutation in a Family Affected by Early-Onset Osteoporosis

(A and B) Pedigree of the family with autosomal-dominant early-onset osteoporosis (A) and chromatogram of the identified heterozygous WNT1 substitution p.Arg235Trp (B). Note that individual IV:2 has the p.Arg235Trp variant but is too young to be symptomatic.

(C) Analysis of bone microarchitecture. Bone microarchitecture of the distal radius as assessed by high-resolution peripheral quantitative CT (XtremeCT, Scanco Medical, Switzerland) is observed in the family harboring the dominant heterozygous p.Arg235Trp substitution. Combined bone loss affecting both the cortical and the trabecular compartments was detected in family members with heterozygous p.Arg235Trp changes, but not in unaffected family members.

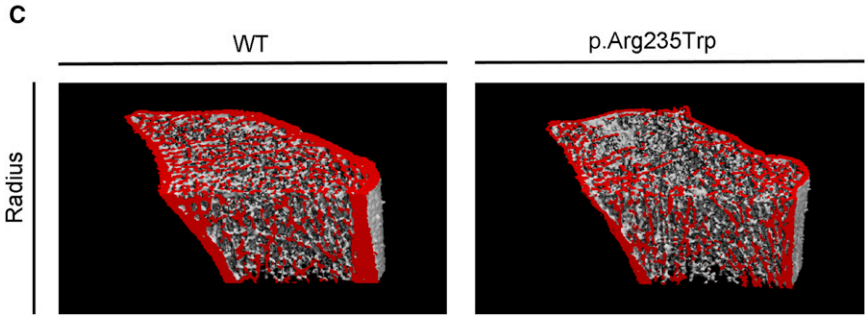

Because WNT is roughly divided into two nearly autonomous domains,[28] the remaining regions, including the site 2 "index finger" Fz-CRD binding site and the region proposed to engage Lrp5/6, would remain intact.[26] Thus, this mutation could potentially allow WNT1 to retain some binding to Fz in a similar fashion to the "mini-Wnt,"[26] but not produce a signal, thereby converting WNT1 into a dominant-negative antagonist. This represents an attractive model-based hypothesis for future functional work. Collectively, both the p.Arg235Trp and the p.Gly177Cys substitutions would certainly appear to be deleterious to WNT structure given their positions in core regions of the molecule; this is in contrast to surface mutants, which would generally not exert such structural destabilization. It is of interest that in addition to the early onset in the family affected by osteoporosis caused by the heterozygous p.Arg235Trp substitution, an early onset of reduced bone mineral density without fractures was also observed in one of the heterozygous carriers of a recessive *WNT1* mutation. Hence, the p.Arg235Trp substitution does not necessarily have to exert a dominant-negative effect. Screening of larger cohorts of persons with early-onset osteoporosis is needed for determining the frequency of predisposing *WNT1* variants.

WNT1 was described as an important regulator of brain development in mice.[27] We determined that *Wnt1* is expressed in bone tissue as well and provide evidence that the osteoblast lineage is a site of expression. Although their exact expression patterns during osteoblast differentiation are not yet known, multiple lines of evidence suggest a key role for *LRP5* and *LRP6* in cell-fate decision, proliferation, and differentiation of osteoblast lineage cells.[29] It is interesting to note that heterozygous loss of WNT3A and WNT5A leads to reduced trabecular bone mineral density to an extent similar to that of homozygous loss of WNT10B.[30,31] Furthermore, *WNT16* was recently described to especially influence

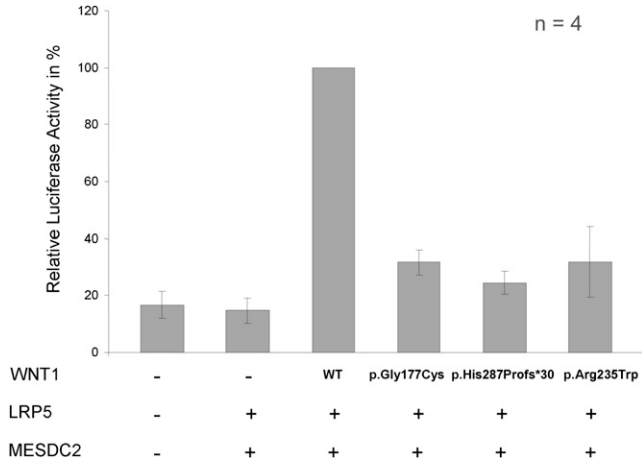

Figure 4. Functional Analysis of *WNT1* Mutations

Dual luciferase reporter assay measuring the canonical WNT signaling activity in HEK293T cells after coexpression of *LRP5*, *MESDC2*, and WT or mutant *WNT1* variants (encoding p.Gly177Cys, p.His287Profs*30, or p.Arg235Trp) or *LacZ*-pcDNA3 (pcDNA3) as negative controls. The graph displays relative luciferase activity (average and SDs) of four independent experiments, which were performed in triplicate each time.

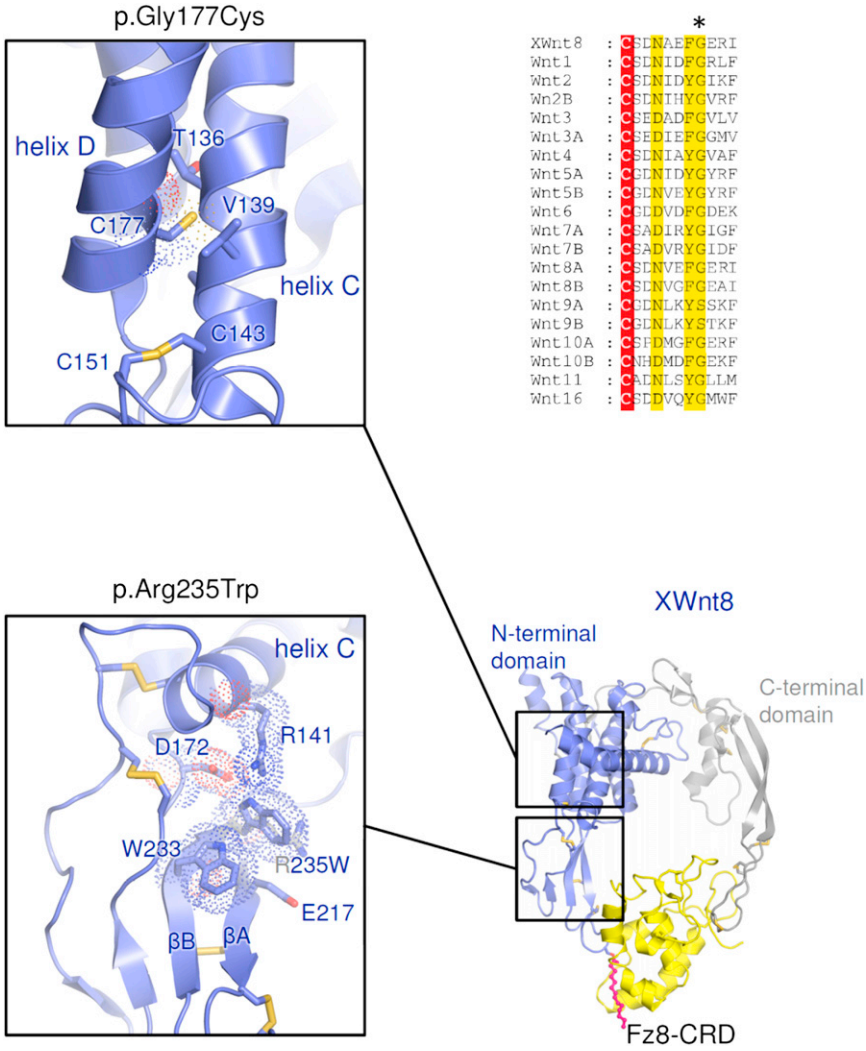

Figure 5. Consequences of *WNT1* Mutations on Crystal Structure
Modeling of the recessive WNT1 p.Gly177Cys and dominant p.Arg235Trp substitutions. The highly conserved Gly at position 177 (top right panel) allows close packing of helices C and D within the Wnt 7 α-helical core. The mutant Cys177 side chain is likely to clash with helix D, impairing the helix C and D interface and destabilizing the Wnt1 core. Arg235 is located within the AB β-hairpin, and the Trp side chain of the p.Arg235Trp mutant is likely to clash with the Trp233, Arg141, and Asp172 side chains, destabilizing the AB β-hairpin and Fz-ECD binding site. The altered protein could retain Fz and LRP5/6 binding but lose its ability to activate signaling, resulting in a dominant-negative effect.

cortical bone in a human genome-wide association study (GWAS) and in a knockout mouse model.[32,33] Our analysis of bone structure in several individuals with *WNT1* mutations revealed a similar cortical thinning and reduced trabecular density (Figure 3C). Currently, no data on the skeletal phenotype of *Wnt1*-deficient or -overexpressing mice are available, which might be due to the fact that the focus has been restricted to the role of WNT1 in the CNS and in tumor formation.[34] *WNT1* overexpression in human mesenchymal stem cells was shown to reduce their osteogenic and adipogenic differentiation but to induce osteogenic differentiation in neighboring non-*WNT1*-expressing WT cells.[35] This indicates that depending on the strength of WNT1-induced stimulation of the canonical pathway, WNT1 has a double role in stem cell maintenance and osteogenic differentiation.[35]

Interestingly, a recent GWAS found SNPs located near *WNT1* in chromosomal region 12q13 to be associated with the risk of low bone mass.[32] This, together with our observations that WNT1 can activate LRP5-mediated WNT signaling and that mutations in *WNT1* cause reduced bone mass and bone fragility, supports the idea that WNT1 is one of the physiological LRP5 ligands inducing canonical WNT signaling in osteoblast-lineage cells. In all individuals with OI due to *WNT1* mutations, therapy with bisphosphonates did not show a substantial effect. This absence of a therapeutic effect is in line with a dysfunction of osteoblasts in individuals carrying *WNT1* mutations but does not apply to children with OI caused by mutations in *COL1A1/2*; in this form of OI, the defect provokes a high turnover state of bone, and a positive effect is observed when osteoclast function is blocked with bisphosphonates.

None of the individuals harboring heterozygous or homozygous *WNT1* mutations had ataxia, other signs of cerebellar dysfunction, or intellectual disability; the only exception was family 1 individual V:2, who presented with brain malformation and developmental delay. Further studies of individuals with mutations in *WNT1* and osteopenic bone diseases will be necessary in the future for establishing whether neurologic complications can be associated in individuals with *WNT1* mutations. In contrast, *Wnt1*-knockout mice and the spontaneous swaying (*sw*) mutant show variable hypoplasia of the cerebellum and midbrain structures, respectively, leading to ataxia in surviving animals.[27,36] One explanation for this discrepancy could be a milder effect of the human mutations. However, our in vitro experiments clearly showed a loss of the ability of the missense and the frameshift variants to induce canonical WNT signaling. The p.Glu189* nonsense change astonishingly truncates the protein exactly in the same position as does the murine *sw* mutation, thus proving its loss-of-function effect.[36] An

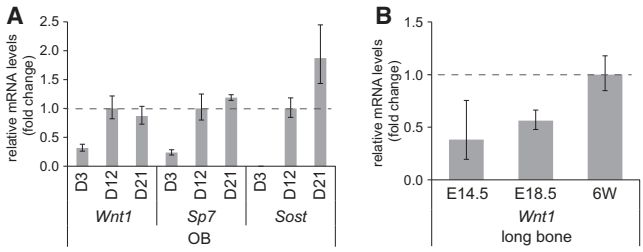

Figure 6. Expression of *Wnt1* in Cultured Osteoblasts and Long Bones

Wnt1 expression analysis by quantitative PCR.
(A) With advancing differentiation, in vitro cultured calvarial osteoblasts show moderately increasing *Wnt1* expression. Osteoblast differentiation markers *Sp7* and *Sost* prove efficient differentiation of osteoblast cultures used for measurement of *Wnt1* expression.
(B) Quantitative *Wnt1* mRNA analysis in long bones shows enhanced expression with increasing age from embryonic day 14.5 (E14.5) to postnatal week 6 (6W). Error bars represent SDs; n=3 for each specimen analyzed.

alternative explanation could be that in the cocktail of WNT proteins during brain development, loss of WNT1 leads to a critical bottleneck situation in mice, but not in humans.

Our finding that homozygous and heterozygous variants in *WNT1* predispose to low-bone-mass phenotypes and bone fragility might facilitate the use of more effective therapeutic strategies. In this context, it is interesting to note that the pharmacological block of WNT-signaling antagonists, such as sclerostin, is currently under investigation in clinical trials.[18] The findings presented in our paper provide additional evidence that this might be an effective therapeutic option in these individuals with low-bone-mass phenotypes.

Supplemental Data

Supplemental Data include one figure and four tables and can be found with this article online at http://www.cell.com/AJHG.

Acknowledgments

We are grateful to all family members who participated in this study, to Esther Milz for excellent technical assistance, and to Karin Boss for critically reading the manuscript. We want to thank Claus-Eric Ott for help with cDNAs and Boi-Dinh Chung-Ueck for kindly providing expression vectors. This work was supported by German Federal Ministry of Education and Research grants 01GM1211A (E-RARE network CRANIRARE-2), 01GM1109C (national rare disease network Forschungsverbund Ausgewählter Craniofacialer Entwicklungsstörungen) to B.W., and 01EC1006A (Molecular Pathogenesis of Osteoporosis) to U.K. and S.M., by TÜBITAK grant 112S398 (E-RARE network CRANIRARE-2) to H.K., and by National Institute of Child Health and Human Development (National Institutes of Health) Intramural Research Program funding to S.L. and J.C.M. M.S. holds a Doc female forte scholarship from Austria and is a member of the Berlin-Brandenburg School for Regenerative Therapies.

Received: January 23, 2013
Revised: February 25, 2013
Accepted: February 27, 2013
Published: March 14, 2013

Web Resources

The URLs for data presented herein are as follows:

Ensembl, http://www.ensembl.org/index.html
NCBI, http://www.ncbi.nlm.nih.gov/
NHLBI Exome Sequencing Project Exome Variant Server (EVS), http://evs.gs.washington.edu/EVS/
Online Mendelian Inheritance in Man (OMIM), http://www.omim.org/
PolyPhen-2, http://genetics.bwh.harvard.edu/pph2/
RefSeq, http://www.ncbi.nlm.nih.gov/RefSeq
UCSC Genome Browser, http://genome.ucsc.edu/index.html
UniProt, http://www.uniprot.org/

References

1. Forlino, A., Cabral, W.A., Barnes, A.M., and Marini, J.C. (2011). New perspectives on osteogenesis imperfecta. Nat Rev Endocrinol *7*, 540–557.
2. Marini, J.C., Forlino, A., Cabral, W.A., Barnes, A.M., San Antonio, J.D., Milgrom, S., Hyland, J.C., Körkkö, J., Prockop, D.J., De Paepe, A., et al. (2007). Consortium for osteogenesis imperfecta mutations in the helical domain of type I collagen: regions rich in lethal mutations align with collagen binding sites for integrins and proteoglycans. Hum. Mutat. *28*, 209–221.
3. Morello, R., Bertin, T.K., Chen, Y., Hicks, J., Tonachini, L., Monticone, M., Castagnola, P., Rauch, F., Glorieux, F.H., Vranka, J., et al. (2006). CRTAP is required for prolyl 3- hydroxylation and mutations cause recessive osteogenesis imperfecta. Cell *127*, 291–304.
4. Cabral, W.A., Chang, W., Barnes, A.M., Weis, M., Scott, M.A., Leikin, S., Makareeva, E., Kuznetsova, N.V., Rosenbaum, K.N., Tifft, C.J., et al. (2007). Prolyl 3-hydroxylase 1 deficiency causes a recessive metabolic bone disorder resembling lethal/severe osteogenesis imperfecta. Nat. Genet. *39*, 359–365.
5. Christiansen, H.E., Schwarze, U., Pyott, S.M., AlSwaid, A., Al Balwi, M., Alrasheed, S., Pepin, M.G., Weis, M.A., Eyre, D.R., and Byers, P.H. (2010). Homozygosity for a missense mutation in SERPINH1, which encodes the collagen chaperone protein HSP47, results in severe recessive osteogenesis imperfecta. Am. J. Hum. Genet. *86*, 389–398.
6. van Dijk, F.S., Nesbitt, I.M., Zwikstra, E.H., Nikkels, P.G., Piersma, S.R., Fratantoni, S.A., Jimenez, C.R., Huizer, M., Morsman, A.C., Cobben, J.M., et al. (2009). PPIB mutations cause severe osteogenesis imperfecta. Am. J. Hum. Genet. *85*, 521–527.
7. Lapunzina, P., Aglan, M., Temtamy, S., Caparrós-Martín, J.A., Valencia, M., Letón, R., Martínez-Glez, V., Elhossini, R., Amr, K., Vilaboa, N., and Ruiz-Perez, V.L. (2010). Identification of a frameshift mutation in Osterix in a patient with recessive osteogenesis imperfecta. Am. J. Hum. Genet. *87*, 110–114.
8. Becker, J., Semler, O., Gilissen, C., Li, Y., Bolz, H.J., Giunta, C., Bergmann, C., Rohrbach, M., Koerber, F., Zimmermann, K., et al. (2011). Exome sequencing identifies truncating

mutations in human SERPINF1 in autosomal-recessive osteogenesis imperfecta. Am. J. Hum. Genet. *88*, 362–371.
9. Alanay, Y., Avaygan, H., Camacho, N., Utine, G.E., Boduroglu, K., Aktas, D., Alikasifoglu, M., Tuncbilek, E., Orhan, D., Bakar, F.T., et al. (2010). Mutations in the gene encoding the RER protein FKBP65 cause autosomal-recessive osteogenesis imperfecta. Am. J. Hum. Genet. *86*, 551–559.
10. Martínez-Glez, V., Valencia, M., Caparrós-Martín, J.A., Aglan, M., Temtamy, S., Tenorio, J., Pulido, V., Lindert, U., Rohrbach, M., Eyre, D., et al. (2012). Identification of a mutation causing deficient BMP1/mTLD proteolytic activity in autosomal recessive osteogenesis imperfecta. Hum. Mutat. *33*, 343–350.
11. Asharani, P.V., Keupp, K., Semler, O., Wang, W., Li, Y., Thiele, H., Yigit, G., Pohl, E., Becker, J., Frommolt, P., et al. (2012). Attenuated BMP1 function compromises osteogenesis, leading to bone fragility in humans and zebrafish. Am. J. Hum. Genet. *90*, 661–674.
12. Shaheen, R., Alazami, A.M., Alshammari, M.J., Faqeih, E., Alhashmi, N., Mousa, N., Alsinani, A., Ansari, S., Alzahrani, F., Al-Owain, M., et al. (2012). Study of autosomal recessive osteogenesis imperfecta in Arabia reveals a novel locus defined by TMEM38B mutation. J. Med. Genet. *49*, 630–635.
13. Puig-Hervás, M.T., Temtamy, S., Aglan, M., Valencia, M., Martínez-Glez, V., Ballesta-Martínez, M.J., López-González, V., Ashour, A.M., Amr, K., Pulido, V., et al. (2012). Mutations in *PLOD2* cause autosomal-recessive connective tissue disorders within the Bruck syndrome—osteogenesis imperfecta phenotypic spectrum. Hum. Mutat. *33*, 1444–1449.
14. Mann, V., and Ralston, S.H. (2003). Meta-analysis of COL1A1 Sp1 polymorphism in relation to bone mineral density and osteoporotic fracture. Bone *32*, 711–717.
15. Raisz, L.G. (1999). Physiology and pathophysiology of bone remodeling. Clin. Chem. *45*, 1353–1358.
16. Ralston, S.H., and Uitterlinden, A.G. (2010). Genetics of osteoporosis. Endocr. Rev. *31*, 629–662.
17. Perdu, B., and Van Hul, W. (2010). Sclerosing bone disorders: too much of a good thing. Crit. Rev. Eukaryot. Gene Expr. *20*, 195–212.
18. Rachner, T.D., Khosla, S., and Hofbauer, L.C. (2011). Osteoporosis: now and the future. Lancet *377*, 1276–1287.
19. Ai, M., Heeger, S., Bartels, C.F., and Schelling, D.K.; Osteoporosis-Pseudoglioma Collaborative Group. (2005). Clinical and molecular findings in osteoporosis-pseudoglioma syndrome. Am. J. Hum. Genet. *77*, 741–753.
20. Gong, Y., Slee, R.B., Fukai, N., Rawadi, G., Roman-Roman, S., Reginato, A.M., Wang, H., Cundy, T., Glorieux, F.H., Lev, D., et al.; Osteoporosis-Pseudoglioma Syndrome Collaborative Group. (2001). LDL receptor-related protein 5 (LRP5) affects bone accrual and eye development. Cell *107*, 513–523.
21. Laine, C.M., Chung, B.D., Susic, M., Prescott, T., Semler, O., Fiskerstrand, T., D'Eufemia, P., Castori, M., Pekkinen, M., Sochett, E., et al. (2011). Novel mutations affecting LRP5 splicing in patients with osteoporosis-pseudoglioma syndrome (OPPG). Eur. J. Hum. Genet. *19*, 875–881.
22. Boutroy, S., Bouxsein, M.L., Munoz, F., and Delmas, P.D. (2005). In vivo assessment of trabecular bone microarchitecture by high-resolution peripheral quantitative computed tomography. J. Clin. Endocrinol. Metab. *90*, 6508–6515.
23. Kamphans, T., and Krawitz, P.M. (2012). GeneTalk: an expert exchange platform for assessing rare sequence variants in personal genomes. Bioinformatics *28*, 2515–2516.
24. Emsley, P., Lohkamp, B., Scott, W.G., and Cowtan, K. (2010). Features and development of Coot. Acta Crystallogr. D Biol. Crystallogr. *66*, 486–501.
25. Chen, V.B., Arendall, W.B., 3rd, Headd, J.J., Keedy, D.A., Immormino, R.M., Kapral, G.J., Murray, L.W., Richardson, J.S., and Richardson, D.C. (2010). MolProbity: all-atom structure validation for macromolecular crystallography. Acta Crystallogr. D Biol. Crystallogr. *66*, 12–21.
26. Janda, C.Y., Waghray, D., Levin, A.M., Thomas, C., and Garcia, K.C. (2012). Structural basis of Wnt recognition by Frizzled. Science *337*, 59–64.
27. McMahon, A.P., and Bradley, A. (1990). The Wnt-1 (int-1) proto-oncogene is required for development of a large region of the mouse brain. Cell *62*, 1073–1085.
28. Bazan, J.F., Janda, C.Y., and Garcia, K.C. (2012). Structural architecture and functional evolution of Wnts. Dev. Cell *23*, 227–232.
29. Monroe, D.G., McGee-Lawrence, M.E., Oursler, M.J., and Westendorf, J.J. (2012). Update on Wnt signaling in bone cell biology and bone disease. Gene *492*, 1–18.
30. Bennett, C.N., Longo, K.A., Wright, W.S., Suva, L.J., Lane, T.F., Hankenson, K.D., and MacDougald, O.A. (2005). Regulation of osteoblastogenesis and bone mass by Wnt10b. Proc. Natl. Acad. Sci. USA *102*, 3324–3329.
31. Takada, I., Mihara, M., Suzawa, M., Ohtake, F., Kobayashi, S., Igarashi, M., Youn, M.Y., Takeyama, K., Nakamura, T., Mezaki, Y., et al. (2007). A histone lysine methyltransferase activated by non-canonical Wnt signalling suppresses PPAR-gamma transactivation. Nat. Cell Biol. *9*, 1273–1285.
32. Estrada, K., Styrkarsdottir, U., Evangelou, E., Hsu, Y.H., Duncan, E.L., Ntzani, E.E., Oei, L., Albagha, O.M., Amin, N., Kemp, J.P., et al. (2012). Genome-wide meta-analysis identifies 56 bone mineral density loci and reveals 14 loci associated with risk of fracture. Nat. Genet. *44*, 491–501.
33. Zheng, H.F., Tobias, J.H., Duncan, E., Evans, D.M., Eriksson, J., Paternoster, L., Yerges-Armstrong, L.M., Lehtimäki, T., Bergström, U., Kähönen, M., et al. (2012). WNT16 influences bone mineral density, cortical bone thickness, bone strength, and osteoporotic fracture risk. PLoS Genet. *8*, e1002745.
34. Ellisor, D., Rieser, C., Voelcker, B., Machan, J.T., and Zervas, M. (2012). Genetic dissection of midbrain dopamine neuron development in vivo. Dev. Biol. *372*, 249–262.
35. Liu, G., Vijayakumar, S., Grumolato, L., Arroyave, R., Qiao, H., Akiri, G., and Aaronson, S.A. (2009). Canonical Wnts function as potent regulators of osteogenesis by human mesenchymal stem cells. J. Cell Biol. *185*, 67–75.
36. Thomas, K.R., Musci, T.S., Neumann, P.E., and Capecchi, M.R. (1991). Swaying is a mutant allele of the proto-oncogene Wnt-1. Cell *67*, 969–976.